Superficial CD34+ fibroblastic tumor with focal atypical presentation: A case report

JUAN SUN[1], SHENGLIANG HUANG[2] and XIAOQING YANG[3]

[1]Department of Dermatology, Jinan First People's Hospital; Departments of [2]Urology and [3]Pathology, The First Affiliated Hospital of Shandong First Medical University and Shandong Provincial Qianfoshan Hospital, Jinan, Shandong 250014, P.R. China

Received September 20, 2023; Accepted March 5, 2024

DOI: 10.3892/ol.2024.14468

Abstract. Superficial CD34+ fibroblastic tumors (SCPFTs) are rare mesenchymal tumors with distinct morphological features. Although several cases of SCPFT have been reported, a comprehensive understanding of its clinical and biological features necessitates the inclusion of additional cases. The current study presents a case of SCPFT, where morphological observations, immunohistochemical staining and fluorescence *in situ* hybridization (FISH) were performed. Immunohistochemistry revealed diffuse CD34 expression and integrase interactor 1 expression, whilst FISH indicated rearrangement of the PR/SET domain 10 gene. Microscopic assessment demonstrated typical SCPFT pathology, with a focal nodular region showing a high Ki-67 index, suggesting heterogeneity and the potential for local recurrence. The present study also briefly reviews the differential diagnosis of tumors with morphological similarities. It was found that the precise diagnosis of SCPFT relies on the distinctive pathological features, the use of immunohistochemical markers, including CD34 staining, and the differentiation from similar histological lesions.

Introduction

Superficial CD34-positive fibroblastic tumor (SCPFT) is a rare mesenchymal tumor of intermediate malignancy, with reported cases representing a wide range of ages from pediatrics to the elderly, although the highest incidence is among middle-aged people. The preoperative duration typically exceeds 1 year. SCPFT typically manifests as a long-standing, painless mass in the subcutaneous tissue, commonly occurring in the lower limbs, occasionally in the upper limbs and back, and rarely in the neck, chest, axilla, abdominal wall and breast (1). SCPFT was first reported by Carter *et al* (2) in 2014 and then described as a new entity in the 5th edition of the World Health Organization (WHO) classification of soft tissue tumors (3). Clinically, SCPFT presents as a slow-growing, painless, circumscribed mass that mainly occurs in adults, and it generally involves the deep dermis and subcutaneous tissues, showing a predilection for the lower extremities. Grossly, SCPFT sections are firm and yellow-to-tan in color. Microscopically, SCPFTs are composed of spindled to epithelioid cells arranged in a fascicular pattern. The tumor cells show apparent cellular heterogeneity and prominent nucleoli with apparent CD34 positivity (4).

Surgical resection is the optimal treatment for most patients, resulting in a good long-term prognosis. However, patients with positive surgical margins may experience local recurrence, while regional lymph node metastasis is uncommon (1,5). However, more cases are needed for long-term prognostic data to establish reliable indicators. The current report presents a case of a typical SCPFT with morphological, immunophenotypic and molecular characteristics, revealing internal morphological heterogeneity.

Case report

A 43-year-old male patient was admitted to the Shandong Provincial Qianfoshan Hospital (Jinan, China) in October 2022, following the discovery of a tumor in the left perineum. The lesion, initially presenting as a mildly tender mass at the thigh roots near the scrotum 6 months prior, exhibited slow growth without signs of irritation or inflammation. Upon physical examination, a contained solid mass measuring 5.5x4x3 cm was observed. Computed tomography revealed a hypoechoic enclosed mass, measuring 5x3.5x3 cm, at the base of the thigh (Fig. 1A). There were no abnormalities present in the hematological laboratory tests, including peripheral blood cell analysis, coagulation index and blood infection markers. The tumor was surgically excised under general anesthesia, involving complete capsule removal, and the excised tumor exhibited a white-colored, cartilage-like consistency on the cut surface (Fig. 1B).

Correspondence to: Dr Xiaoqing Yang, Department of Pathology, The First Affiliated Hospital of Shandong First Medical University and Shandong Provincial Qianfoshan Hospital, 16766 Jingshi Road, Jinan, Shandong 250014, P.R. China
E-mail: yangxiaoqing@sdfmu.edu.cn

Key words: superficial CD34+ fibroblastic tumor, CD34, immunohistochemistry, integrase interactor 1/SWI/SNF-related matrix-associated actin-dependent regulator of chromatin subfamily B member 1, fluorescence *in situ* hybridization, PR/SET domain 10 rearrangement

The tumor was cut into flat tissue blocks ~2x1.5 cm in size and 0.3 cm in thickness. These tumor blocks were then fixed in a solution containing 10% formaldehyde in 0.01 M phosphate-buffered saline (PBS) for 2 h at room temperature. Following fixation, the tissue blocks were loaded into the Tissue-Tek VIP®6 AI Tissue Processor (Sakura Finetek USA, Inc.) and subsequently embedded in paraffin. Formalin-fixed paraffin-embedded sections were cut using a Leica RM 2155 Rotary Microtome (Leica Microsystems). The subsequent dewaxing process included sequential treatments with xylene, anhydrous ethanol, a decreasing concentration gradient of ethanol (95, 90, 80 and 70%), and water. Following this, the sections were immersed in Harris hematoxylin staining solution for 5 min and then differentiated with 0.3% acid alcohol, before being incubated with 0.6% ammonia. Eosin staining solution was applied for 1-3 min, followed by dehydration with ethanol and xylene. Finally, the samples were mounted with neutral gum to prepare the slides. Postoperative histopathological microscopy revealed that the lesion was confined within the subcutaneous tissue, and at low magnification, the dermis of the skin showed infiltration by tumor cells (Fig. 1C). The tumor displayed sparse-to-moderate cellularity, featuring a densely cellular, basophilic, nodular area at the periphery. Under high magnification, the tumor primarily consisted of spindle-shaped to epithelioid cells, arranged singly or in clusters within a collagenous stroma. The tumor cells exhibited marked nuclear pleomorphism with prominent nucleoli, abundant eosinophilic cytoplasm and occasional multilobed nuclei or intranuclear exudate inclusion bodies. Scattered lymphocytes and eosinophils were observed in the interstitium (Fig. 1D and E). Within the densely populated nodule, the tumor cells displayed the same morphological characteristics but were relatively smaller in size and more tightly arranged compared with other regions (Fig. 1F).

Paraffin sections of 5-μm were loaded into The Discovery ULTRA (Roche Tissue Diagnostics) for automated staining. The automated immunohistochemistry staining process utilized solutions and antibodies from Roche Tissue Diagnostics unless otherwise specified. Initially, slides underwent de-paraffinization with the EZ PREP solution (cat. no. 950-100), followed by antigen retrieval through Heat Induced Epitope Retrieval in Tris-EDTA buffer (cat. no. 950-124) at pH 7.8 and 95˚C for 40 min. Subsequently, primary antibodies were manually applied and incubated at 37˚C for 60 min. The targets were then linked using the OmniMap anti-rabbit (cat. no. 760-4311) and OmniMap anti-mouse (cat. no. 760-4310) HRP-conjugated secondary antibodies. Visualization of the different targets was achieved through DAB and H_2O_2 (cat. no. 760-159). Finally, tissue slides were counterstained with hematoxylin and mounted using a xylene-based mounting medium. The following ready-to-use primary antibodies were utilized: Cytokeratin [anion exchanger (AE)1/AE3; cat. no. Kit-0009], epithelial membrane antigen (EMA; cat. no. Kit-0011), ERG (cat. no. RMA-0748), STAT6 (cat. no. RMA-0845), CD34 (cat. no. MAB-1076), smooth muscle actin (SMA; cat. no. MAB-0890), Desmin (cat. no. MAB-0766), S100 protein (cat. no. MAB-0697), CD10 (cat. no. MAB-0668), CD117 (cat. no. Kit-0029), discovered on GIST-1 (DOG1; cat. no. MAB-0851), integrase interactor 1 (INI1)/SWI/SNF-related matrix-associated actin-dependent regulator of chromatin subfamily B member 1 (SMARCB1) (cat. no. MAB-0696), anaplastic lymphoma kinase (ALK; cat. no. MAB-0848) and Ki-67 (cat. no. MAB-0672). All antibodies were purchased from MaximBiotech, Inc. The tumor cells exhibited strong positive staining for CD34 in a diffuse pattern (Fig. 2A). Nuclear expression of INI1/SMARCB1 was evident in all cases (Fig. 2B). The Ki-67 labeling index was ~5% in most areas and ~20% in the focal cell-dense regions (Fig. 2C and D). Furthermore, the tumor cells displayed negative staining for AE1/AE3, CD117, STAT6, DOG1, SMA, ALK, Desmin, CD10, ERG, EMA and S-100 expression (Figs. S1 and S2).

For fluorescence *in situ* hybridization (FISH), a commercial TGFBR3-MGEA5 Dual Fusion/Translocation FISH probe (cat. no. F.01228-01) and PRDM10 Break Apart FISH probe (cat. no. F.01377-01) were obtained from Guangzhou Anbiping Medical Laboratory Co., Ltd. The PRDM10 probe utilized two custom-labeled FISH DNA probes to label the PRDM10 gene flanks on chromosome 11. Specifically, the BAC clone D11S1083 (366 kb), positioned centromeric to PRDM10, was labeled with FITC dUTP, while the BAC clone RH104271 (189 kb), located telomeric to PRDM10, was labeled with 5(6)-TRITC dUTP. In the case of the TGFBR3-MGEA5 Dual Fusion/Translocation FISH Probe, the BAC clone BV444963-STSG24458 (872 kb) was labeled with FITC dUTP to identify the TGFBR3 gene, and the BAC clone SHGC153008-D10S2456 (765 kb) was labeled with 5(6)-TRITC dUTP for identifying the MGEAS gene.

Paraffin sections of 4 μm were dewaxed and hydrated. Chromosomal DNA was denatured on the slides in a 70% formamide-2XSSC solution at 68-70˚C for 2 min. Subsequently, the slides were dehydrated and air-dried. The hybridization mixture, containing DNA probe at a concentration of 20-50 μg/ml, was added to the slide and covered with a cover slip. Subsequently, the slides were incubated in a moist plastic chamber at 37˚C for 6-12 h. After incubation, the slides were washed and dried before being immersed in blocking buffer (1X PBS, 0.1% Triton-100) for 2 min. Following this, the slides were rinsed in PBS for 5 min at room temperature. The semi-dried slides were then treated with 100 μl of 1:100 rabbit antibiotin antibody and incubated in a humidity chamber at 37˚C for 5 min. Subsequently, the slides were washed with PBS and immersed in 100 μl diluted antibody (FITC-conjugated goat anti-rabbit antibody at a ratio of 1:100 in dilution buffer). Slides were then incubated in the humidity chamber at 37˚C for 30-60 min. After incubation, the slides were washed again, and 60 μl of an antifade solution (composed of p-phenylenediamine at a concentration of 10 mg/ml, 90% glycerol and propidium iodide at 1 μg/ml as a counterstain) was added to each slide. The slides were observed under fluorescence microscope (BM4000B, Leica Microsystems GmbH).

FISH analysis revealed a positive rearrangement of the PRDM10 gene (Fig. 2E), whilst TGFBR3/MGEA5 showed negative results (Fig. 2F). These findings aligned with a diagnosis of SCPFT. Post-surgery, the patient exhibited a rapid recovery. There is no clear academic consensus on the optimal follow-up time after SCPFT. The patient will be monitored every 6 months during the first postoperative year and annually thereafter. So far, the patient has not had recurrence or metastasis.

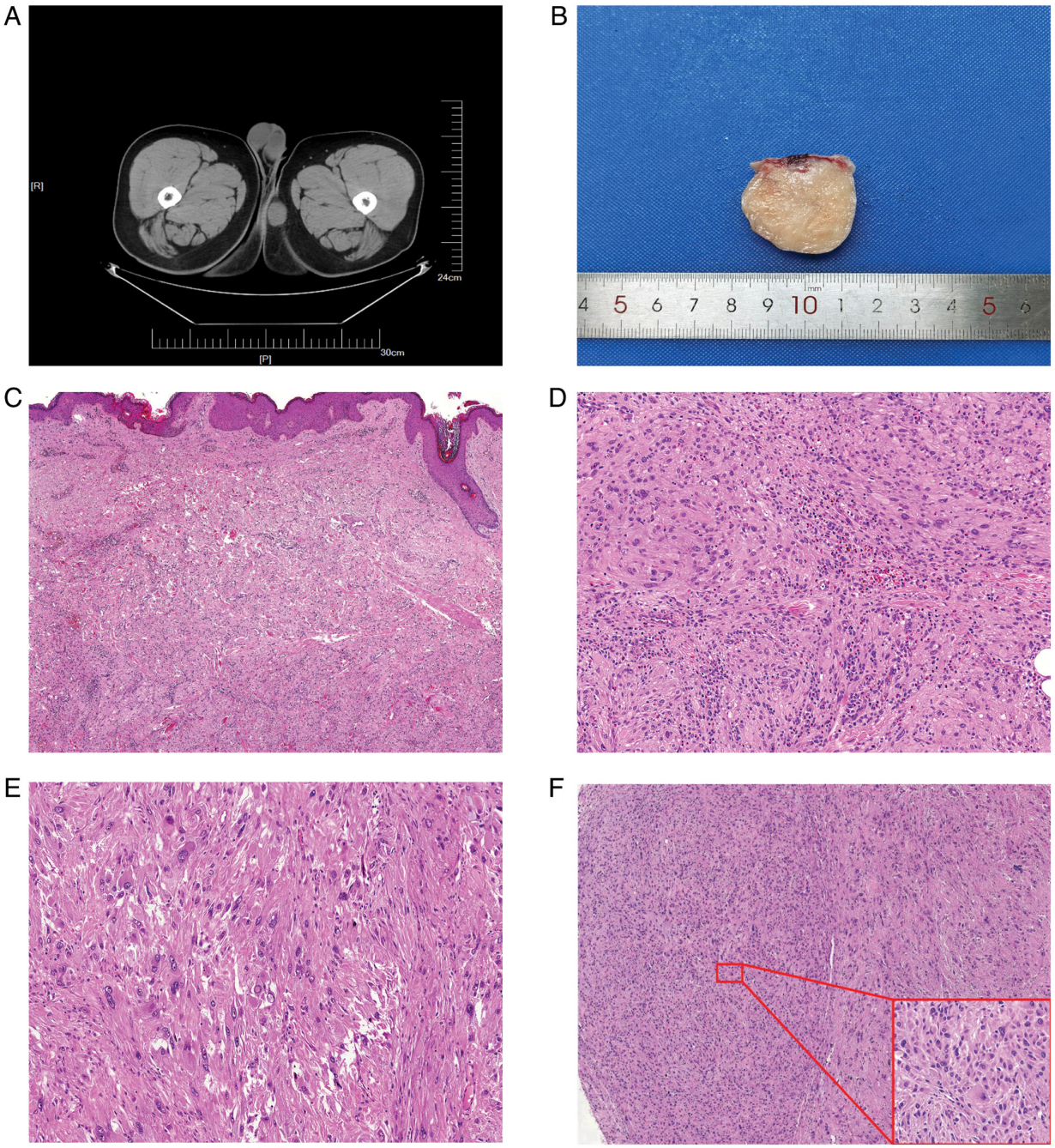

Figure 1. (A) Gross appearance of the tumor specimen presenting with a grayish-white color in section and a tough texture. (B) Computed tomography image demonstrating a hypoechoic, well-demarcated mass situated at the base of the thigh. (C) Tumor cells situated beneath the dermis and exhibiting local infiltration into the dermis (HE, x100 magnification). (D) Tumor cells arranged in bundles, accompanied by eosinophils and lymphocytes in the background (HE, x200 magnification). (E) Tumor cells with distinct nucleoli, with visible intranuclear inclusion bodies (HE, x400 magnification). (F) Tumor margins featuring cell-rich areas, as depicted in the inset (HE, x400 magnification), showing tumor cells with abundant cytoplasm, atypical nuclei and a small size (HE, x100 magnification). HE, hematoxylin and eosin.

Discussion

SCPFT was initially identified and characterized in 2014 by Carter *et al* (2) in an assessment of 18 cases. The tumors were observed in the superficial subcutaneous layer, displaying notable pleomorphic cells, a low mitotic index, absence of necrosis and widespread strong positivity for CD34 in immunohistochemical staining. Carter *et al* designated this distinctive entity as SCPFT. In the 2020 revision of the WHO Classification of Soft Tissue and Bone Tumors, SCPFT was acknowledged as a novel tumor (3). SCPFT has garnered growing attention from pathologists, resulting in a rise in the number of published cases. Presently, ~150 cases of SCPFTs have been documented in the English-language literature (5-15).

Clinically, SCPFT predominantly affects young adults spanning an age range of 8-85 years, with a slight prevalence in males (5,7). The primary sites of SCPFT occurrence are commonly the lower limbs, particularly the thighs, along with other locations such as the calves, groin, foot, Achilles tendon, shoulder, vulva, neck, knee, buttocks and arms. The majority of

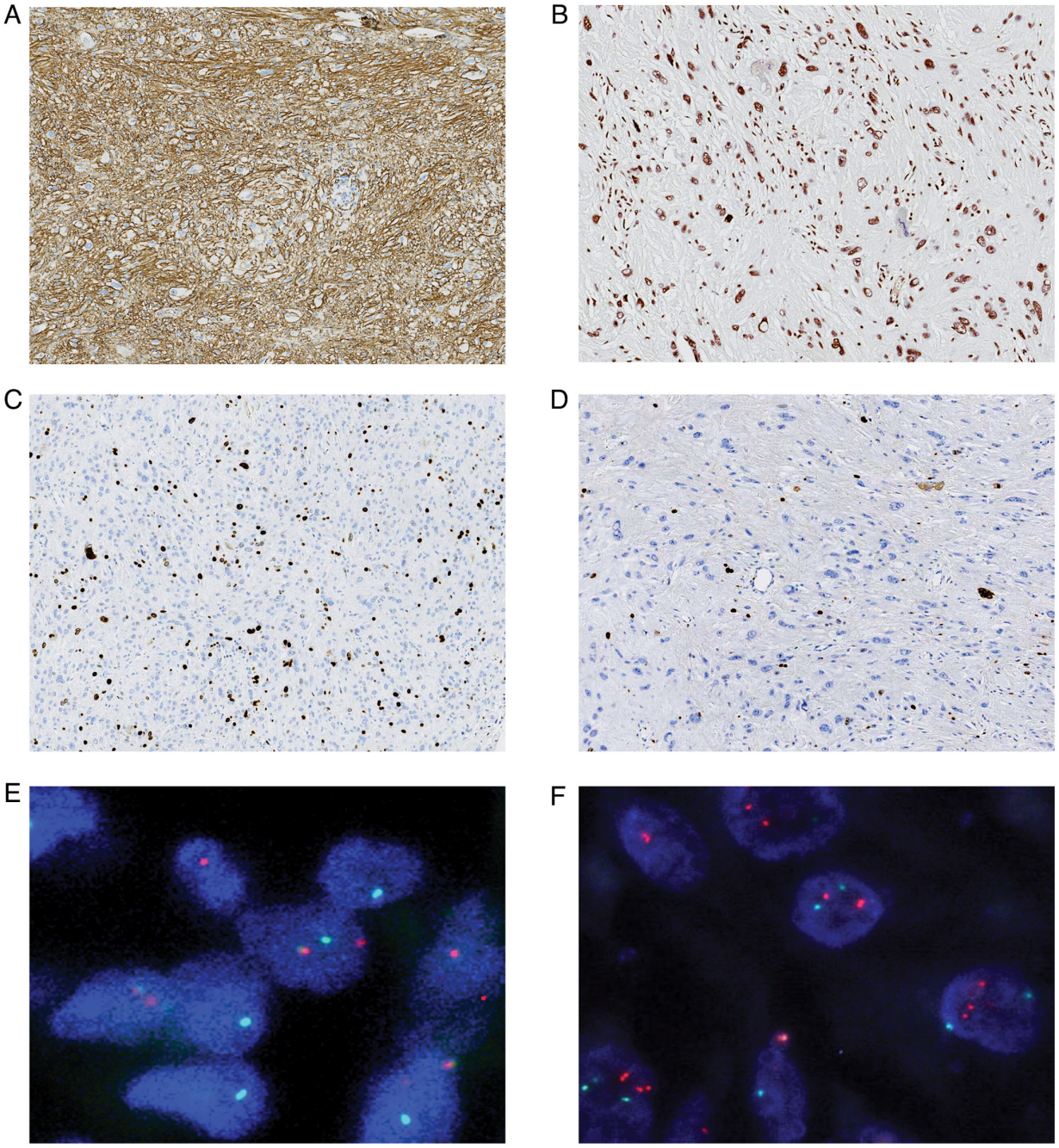

Figure 2. (A) Immunohistochemical staining demonstrating tumor CD34 diffuse cytoplasmic positivity (x200 magnification). (B) Positive nuclear staining for integrase interactor 1 observed via immunohistochemical analysis (x200 magnification). (C) Cell-rich region displaying high Ki-67 expression (x200 magnification). (D) Tumor cells outside the cell-rich nodules with very low expression of Ki-67 (x200 magnification). (E) Dual-color break-apart probe analysis indicating a rearrangement in the PR/SET domain 10 gene (x1,000 magnification) and (F) transforming growth factor β receptor 3/MGEA5 dual-color fusion probe showing MGEA5 is negative for gene breaks (x1,000 magnification).

cases are situated in the deep dermis to the superficial subcutis. Grossly, SCPFTs vary in size from 1.2-10 cm, typically exhibiting a circumscribed border but occasionally infiltrating surrounding soft tissues (16). Microscopically, SCPFTs consist of spindled to epithelioid cells arranged in fascicles or storiform formations. The cells exhibit prominent eosinophilic cytoplasm, notable nuclear pleomorphism with prominent macronucleoli and occasional pseudoinclusions. The interstitium displays branching capillaries and scattered lymphocytes, mast cells and foam cells. Mitotic figures are exceedingly rare (<1/50 high-power fields). Immunohistochemically, SCPFT cells consistently exhibit diffuse and strong positivity for CD34. Recently, synaptic cell adhesion molecule 3 has been identified as a sensitive marker expressed in 95% (56/59 cases) of SCPFT (17). The Ki-67 index is generally low in SCPFT, typically <5% (7).

In 2015, Hofvander *et al* identified recurrent PRDM10 gene fusions for the first time in 3/28 cases of undifferentiated pleomorphic sarcoma (UPS) with a morphological resemblance to SCPFT (18). It was hypothesized that these cases represented a subset of low-grade UPS. Subsequent studies have assessed the relationship between SCPFT and PRDM10-STT,

highlighting their overlapping features and leaning toward considering them as part of the same spectrum (5,17,19). Due to the presence of marked cellular pleomorphism and nuclear atypia, an accurate diagnosis of SCPFT necessitates the exclusion of superficially located and high-grade sarcomas with morphological similarities (19).

The principal differential diagnoses include atypical fibrous histiocytoma (AFH), pleomorphic hyalinizing angiectatic tumor (PHAT), atypical fibroxanthoma (AFX), epithelioid sarcoma (EpS), UPS, pleomorphic dermal sarcoma (PDS) and myxoinflammatory fibroblastic sarcoma (MIFS). AFH typically exhibits a classic fibrous histiocytoma background interspersed with a population of atypical cells displaying nuclear hyperchromasia and prominent nucleoli, often with abundant cytoplasm. Dermal collagen at the tumor margins and pigmentation of the basal layer aid distinguishes AFH from SCPFT. Although AFH tumor cells may express CD34, it is usually focal and weak, and they generally do not express cytokeratins (20,21). PHAT shares many common features with SCPFT, including a superficial location, marked pleomorphism of tumor cells, inconspicuous mitotic activity, pseudo-inclusions in the nucleus and diffuse $CD34^+$ staining. However, PHAT has distinctive features, such as thick-walled ectopic vessels with marked perivascular hyalinization (22). AFX typically occurs on sun-exposed skin in elderly patients, featuring highly pleomorphic cells with hyperchromatic nuclei, atypical mitoses and abundant cytoplasm, commonly arranged in a spindly architecture. Multinucleated giant cells and solar elastosis are often present in AFX specimens. AFX stains positive for several markers, including CD10 and p53, but is negative or focally positive for CD34 (23). EpS shares certain immunophenotypic similarities with SCPFT, exhibiting diffuse or patchy expression of cytokeratin and CD34 in ~50% of cases. However, EpS is characterized by epithelioid to spindled cells with central pseudogranulomatous architecture in the classic type, and predominant epithelioid and rhabdoid cells in the proximal type, distinguishing it from SCPFT. Loss of nuclear expression of SMARCB1 is a hallmark feature of EpS, present in the vast majority of cases (24). UPS typically occurs in middle-aged and older patients, originating in deeper tissues and morphologically showing marked pleomorphism, heterogeneity and aberrant mitosis. UPS may express CD34 focally, but not diffusely, in contrast to SCPFTs (25). PDS may infiltrate the subcutis, potentially causing confusion with SCPFT. PDS exhibits true pleomorphism and heterogeneity, with common appearances of mitotic figures and necrosis, similar to AFX. PDS expresses CD10 but not CD34 diffusely (26). Finally, MIFS typically exhibits a multinodular growth pattern with a variable combination of three morphologic zones: Myxoid, hyalinized and inflammatory. MIFS tumor cells can range from plump spindle cells to histiocytoid or epithelioid cells, featuring enlarged basophilic or eosinophilic macronucleoli reminiscent of virallyinfected nuclei. Variable expression of CD34 is not uncommon in MIFS and can be prominent in certain cases. Certain subset cases may involve molecular genetic alterations, such as MGEA5 or BRAF rearrangements (27).

SCPFT is considered to originate from $CD34^+$ fibroblasts, which are a subset of fibroblasts and are assumed to be mesenchymal stem cells. A series of fibroblastic tumors that exhibit $CD34^+$ activity, including leiomyosarcoma and primary fibrosarcoma, are believed to originate from $CD34^+$ fibroblasts (28). CD34 is a transmembrane phosphoglycoprotein with a molecular weight of ~115 kDa, which was first discovered on hematopoietic stem and progenitor cells (29). CD34 has also been identified as a marker of several types of non-hematopoietic cells, including fibroblast progenitors and endothelial precursors (30). The exact functions of CD34 proteins remain complex and multifaceted. Researchers have proposed potential roles for CD34 in promoting cell proliferation and preventing cell differentiation (31). Thus, in SCPFT, CD34 maintains a high self-renewal capacity of fibroblasts, which means that they can continuously undergo cell division and generate more cells. On the other hand, CD34 is associated with endothelial progenitor cells and angiogenesis (32).

In the present study, a panel of antibodies was used for immunohistochemical staining to assist in the diagnosis and differential diagnosis. Concurrently, molecular analysis indicated the presence of a PRDM10 gene rearrangement, thereby confirming the diagnosis of SCPFT. While numerous SCPFT cases have been documented, it is important to note two key points in this specific case. Firstly, SCPFT usually develops in the thigh; however, in this instance, the tumor was located near the scrotum in the groin, which is a less common site for SCPFT. Secondly, various regions within the tumor exhibited distinct levels of proliferative activity. Notably, the cell-dense nodules displayed higher proliferative activity compared with other regions, as highlighted by an elevated Ki-67 proliferation index. This demonstrates that intra-tumor heterogeneity and the potential of local recurrence exists in SCPFT, indicating that clinicians should adjust their follow-up strategy to increase the frequency of follow-up visits when required.

In conclusion, the present study describes a case of SCPFT located in the groin, which was confirmed by using immunohistochemistry and FISH. Moreover, tumor heterogeneity was identified in this case. Despite an increasing number of reported SCPFT cases, further accumulation of cases is essential to unravel the intrinsic mechanisms and clinical characteristics of SCPFT.

Acknowledgements

Not applicable.

Funding

No funding was received.

Availability of data and materials

The data generated in the present study may be requested from the corresponding author.

Authors' contributions

JS was the first-visit doctor who designed the study and the main writer of the manuscript.SH was the surgeon who acquired and analyzed the patient's clinical data. XY is a diagnostic pathologist who performed the pathological assessment of the patient and participated in the writing of the manuscript. All authors

have read and approved the final version of the manuscript. JS and SH confirm the authenticity of all the raw data

Ethics approval and consent to participate

The present study was approved by the Medical Ethics Committee of the First Affiliated Hospital of Shandong First Medical University (Jinan, China; approval no. 2023-S434).

Patient consent for publication

Written informed consent was obtained from the patient for publication of this case report and any accompanying images.

Competing interests

The authors declare that they have no competing interests.

References

1. Salah HT, D'Ardis JA, Baek D, Duran J, Schwartz MR, Ayala AG and Ro JY: Case of recurrent superficial CD34-positive fibroblastic tumor. J Cutan Pathol 50: 477-480, 2023.
2. Carter JM, Weiss SW, Linos K, DiCaudo DJ and Folpe AL: Superficial CD34-positive fibroblastic tumor: Report of 18 cases of a distinctive low-grade mesenchymal neoplasm of intermediate (borderline) malignancy. Mod Pathol 27: 294-302, 2014.
3. WHO Classification of Tumours: Soft Tissue and Bone Tumours. IARC Press, France, 2020.
4. Salah HT, D'ardis JA, Baek D, Schwartz MR, Ayala AG and Ro JY: Superficial CD34-positive fibroblastic tumor (SCPFT): A review of pathological and clinical features. Ann Diagn Pathol 58: 151937, 2022.
5. Anderson WJ, Mertens F, Mariño-Enríquez A, Hornick JL and Fletcher CD: Superficial CD34-positive fibroblastic tumor: A clinicopathologic, immunohistochemical, and molecular study of 59 cases. Am J Surg Pathol 46: 1329-1339, 2022.
6. Li W, Molnar SL, Mott M, White E and De Las Casas LE: Superficial CD34-positive fibroblastic tumor: Cytologic features, tissue correlation, ancillary studies, and differential diagnosis of a recently described soft tissue neoplasm. Diagn Cytopathol 44: 926-930, 2016.
7. Lao IW, Yu L and Wang J: Superficial CD34-positive fibroblastic tumour: A clinicopathological and immunohistochemical study of an additional series. Histopathology 70: 394-401, 2017.
8. Perret R, Michal M, Carr RA, Velasco V, Švajdler M, Karanian M, Meurgey A, Paindavoine S, Soubeyran I, Coindre JM, *et al*: Superficial CD34-positive fibroblastic tumor and PRDM10-rearranged soft tissue tumor are overlapping entities: A comprehensive study of 20 cases. Histopathology 79: 810-825, 2021.
9. Sood N and Khandelia BK: Superficial CD34-positive fibroblastic tumor: A new entity; case report and review of literature. Indian J Pathol Microbiol 60: 377-380, 2017.
10. Rekhi B, Banerjee D, Gala K and Gulia A: Superficial CD34-positive fibroblastic tumor in the forearm of a middle-aged patient: A newly described, rare soft-tissue tumor. Indian J Pathol Microbiol 61: 421-424, 2018.
11. Hamada T, Katsuki N, Hosokawa Y, Ayano Y and Ikeda M: Additional case of superficial CD34-positive fibroblastic tumor in a Japanese patient. J Dermatol 46: e134-e136, 2019.
12. Batur S, Ozcan K, Ozcan G, Tosun I and Comunoglu N: Superficial CD34 positive fibroblastic tumor: Report of three cases and review of the literature. Int J Dermatol 58: 416-422, 2019.
13. Ding L, Xu WJ, Tao XY, Zhang L and Cai ZG: Clinicopathological features of superficial CD34-positive fibroblastic tumor. World J Clin Cases 9: 2739-2750, 2021.
14. Li SY, Zhang HL and Bai YZ: Superficial CD34-positive fibroblastic tumor on the chest wall of an 8-year-old girl: A case report and literature review. Pediatr Hematol Oncol 38: 602-608, 2021.
15. Mao X, Sun YY, Deng ML, Ma T and Yu L: Superficial CD34-positive fibroblastic tumor: Report of two cases and review of literature. Int J Clin Exp Pathol 13: 38-43, 2020.
16. Andrei V, Haefliger S and Baumhoer D: Superficial mesenchymal tumours expressing epithelial markers on immunohistochemistry: Diagnostic clues and pitfalls. Semin Diagn Pathol 40: 238-245, 2023.
17. Puls F, Carter JM, Pillay N, McCulloch TA, Sumathi VP, Rissler P, Fagman H, Hansson M, Amary F, Tirabosco R, *et al*: Overlapping morphological, immunohistochemical and genetic features of superficial CD34-positive fibroblastic tumor and PRDM10-rearranged soft tissue tumor. Mod Pathol 35: 767-776, 2022.
18. Hofvander J, Tayebwa J, Nilsson J, Magnusson L, Brosjö O, Larsson O, von Steyern FV, Mandahl N, Fletcher CD and Mertens F: Recurre2nt PRDM10 gene fusions in undifferentiated pleomorphic sarcoma. Clin Cancer Res 21: 864-869, 2015.
19. Zhao M, Yin X, He H, Fan Y, Ru G and Meng X: Recurrent PRDM10 fusions in superficial CD34-positive fibroblastic tumors: A clinicopathologic and molecular study of 10 additional cases of an emerging novel entity. Am J Clin Pathol 159: 367-378, 2023.
20. Rayyan MM, Aboushelib M, Sayed NM, Ibrahim A and Jimbo R: Comparison of interim restorations fabricated by CAD/CAM with those fabricated manually. J Prosthet Dent 114: 414-419, 2015.
21. Kaddu S, McMenamin ME and Fletcher CD: Atypical fibrous histiocytoma of the skin: Clinicopathologic analysis of 59 cases with evidence of infrequent metastasis. Am J Surg Pathol 26: 35-46, 2002.
22. Michal M, Kazakov DV, Hadravský L, Agaimy A, Švajdler M, Kuroda N and Michal M: Pleomorphic hyalinizing angiectatic tumor revisited: All tumors manifest typical morphologic features of myxoinflammatory fibroblastic sarcoma, further suggesting 2 morphologic variants of a single entity. Ann Diagn Pathol 20: 40-43, 2016.
23. Gru AA and Cruz DJ: Atypical fibroxanthoma: A selective review. Semin Diagn Pathol 30: 4-12, 2013.
24. Kohashi K, Yamada Y, Hotokebuchi Y, Yamamoto H, Taguchi T, Iwamoto Y and Oda Y: ERG and SALL4 expressions in SMARCB1/INI1-deficient tumors: A useful tool for distinguishing epithelioid sarcoma from malignant rhabdoid tumor. Hum Pathol 46: 225-230, 2015.
25. Kodera K, Hoshino M, Takahashi S, Hidaka S, Kogo M, Hashizume R, Imakita T, Ishiyama M, Ogawa M and Eto K: Surgical management of primary undifferentiated pleomorphic sarcoma of the rectum: A case report and review of the literature. World J Surg Oncol 20: 199, 2022.
26. Ríos-Viñuela E, Serra-Guillén C, Llombart B, Requena C, Nagore E, Traves V, Guillén C, Vázquez D and Sanmartín O: Pleomorphic dermal sarcoma: A retrospective study of 16 cases in a dermato-oncology centre and a review of the literature. Eur J Dermatol 30: 545-553, 2020.
27. Ieremia E and Thway K: Myxoinflammatory fibroblastic sarcoma: Morphologic and genetic updates. Arch Pathol Lab Med 138: 1406-1411, 2014.
28. Díaz-Flores L, Gutiérrez R, García MP, Sáez FJ, Díaz-Flores L Jr, Valladares F and Madrid JF: CD34+ stromal cells/fibroblasts/fibrocytes/telocytes as a tissue reserve and a principal source of mesenchymal cells. Location, morphology, function and role in pathology. Histol Histopathol 29: 831-870, 2014.
29. Tindle RW, Nichols RA, Chan L, Campana D, Catovsky D and Birnie GD: A novel monoclonal antibody BI-3C5 recognises myeloblasts and non-B non-T lymphoblasts in acute leukaemias and CGL blast crises, and reacts with immature cells in normal bone marrow. Leuk Res 9: 1-9, 1985.
30. Brown J, Greaves MF and Molgaard HV: The gene encoding the stem cell antigen, CD34, is conserved in mouse and expressed in haemopoietic progenitor cell lines, brain, and embryonic fibroblasts. Int Immunol 3: 175-184, 1991.
31. Radu P, Zurzu M, Paic V, Bratucu M, Garofil D, Tigora A, Georgescu V, Prunoiu V, Pasnicu C, Popa F, *et al*: CD34-Structure, functions and relationship with cancer stem cells. Medicina (Kaunas) 59: 938, 2023.
32. Krause DS, Fackler MJ, Civin CI and May WS: CD34: Structure, biology, and clinical utility. Blood 87: 1-13, 1996.